11-2001

Local Impurity-Assisted Conductance in Magnetic Tunnel Junctions

Evgeny Y. Tsymbal
University of Nebraska at Lincoln, tsymbal@unl.edu

David G. Pettifor
University of Oxford, david.pettifor@materials.ox.ac.uk

Local impurity-assisted conductance in magnetic tunnel junctions

E. Y. Tsymbal and D. G. Pettifor
Department of Materials, University of Oxford, Parks Road, Oxford OX1 3PH, United Kingdom
(Received 21 May 2001; published 1 November 2001)

Using a simple tight-binding model and the Kubo formula we have calculated the lateral distribution of the tunneling conductance across a magnetic tunnel junction probed by STM. We find that the presence of an isolated impurity within the barrier layer can cause a spike in the conductance distribution, which is in agreement with recent experiments. We show that the local tunneling magnetoresistance (TMR) is very sensitive to the electronic state of the impurity and to the lateral position of the tip. The latter dramatic variation in TMR could be detected by STM.

DOI: 10.1103/PhysRevB.64.212401 PACS number(s): 75.70.Cn, 72.25.−b, 73.40.Gk, 73.40.Rw

Tunneling magnetoresistance (TMR)[1] is the change in electrical resistance that occurs in a magnetic tunnel junction (MTJ) when an applied magnetic field changes the relative alignment of the magnetizations of the two ferromagnetic layers. Recent advances in TMR have demonstrated that high values of magnetoresistance can be achieved at room temperature,[2,3] which has stimulated a tremendous interest in MTJs because of possible applications in magnetic sensors and memories[4] (for reviews on TMR see Refs. 5,6).

Most MTJs are based on an alumina barrier which has an *amorphous* structure. Although nowadays it is possible to grow MTJs with reproducible characteristics, the values of TMR depend significantly on the type and degree of disorder in the amorphous barrier, which results in considerable local variations in the junction resistance.[7] This makes the understanding of intrinsic mechanisms of TMR much more difficult, since the resultant conductance is the average over many local disorder configurations.[8] Therefore, experiments on epitaxial tunnel junctions with *crystalline* insulating barriers could play an important role from the point of view of elucidating the underlying physics which controls the spin polarization of the tunneling current. This would also simplify the first-principles treatment of TMR.[9–11]

Recently, Wulfhekel *et al.*[12] have grown epitaxial single crystalline MTJs using Fe(001) substrates, MgO (001) barriers, and Fe top electrodes. Using scanning tunneling microscopy (STM) they measured lateral scans of the tunneling current and found spikes in the conductance distribution. These spikes were attributed to ballistic electrons tunneling via localized electronic states within the band gap of MgO. The ability to detect localized states in the insulating layer through the top metal film makes the STM technique, along with ballistic electron emission microscopy (BEEM),[13] very attractive for studying the quality of the barriers in MTJs. More importantly, this method has a potential for investigating the influence of local defects and impurities on TMR.

In this paper we elucidate the effect of an isolated impurity within the barrier on the local conductance in a crystalline MTJ probed by STM. We demonstrate that the resonant nature of the impurity-assisted tunneling and the coupling between the impurity and the ferromagnetic electrodes through the barrier control the spin dependence of the conductance. Switching the magnetic alignment of the two electrodes leads to TMR, the magnitude and the sign of which depend strongly on the electronic state of the impurity. The local TMR varies dramatically as the tip scans an area above the impurity atom, which could be observed by STM within a geometry similar to that used by Wulfhekel *et al.*[12]

The fact that the TMR is sensitive to the impurity state can be easily shown within a one-dimensional (1D) tight-binding model. Consider two ferromagnetic metal electrodes (the left and the right) separated by a barrier which contains an impurity. Assume that the exchange-split bands of the ferromagnets are characterized by different on-site potentials, i.e., $E_m^{\uparrow}$ and $E_m^{\downarrow}$. Let E_b and E_i be the on-site atomic energies of the barrier and the impurity, respectively, and E_F be the Fermi energy. We evaluate the spin conductance using the Kubo formula[14,15]

$$\Gamma = \frac{2\hbar}{\pi a^2} \mathrm{Tr}[J\,\mathrm{Im}(G) J\,\mathrm{Im}(G)], \tag{1}$$

where a is the lattice parameter and spin indices have been dropped for simplicity of notation. The local current operator J takes the form

$$J = \frac{ea}{i\hbar}\beta\{|n_1\rangle\langle n_2| - |n_2\rangle\langle n_1|\}, \tag{2}$$

where $|n_1\rangle$ and $|n_2\rangle$ are the orbitals of two nearest-neighbor atoms coupled by the hopping or bond integral $-\beta$. Due to current conservation these two atoms can be chosen arbitrarily. Assuming for simplicity that $\Delta \equiv (E_b - E_F)/\beta \gg 1$, the matrix elements of the Green's function G in Eq. (1) can be evaluated recursively using perturbation theory with respect to Δ^{-1}. The conductance per spin of the 1D MTJ is, then, given by

$$\Gamma = \Gamma_0 \frac{4\pi^2\beta^4\rho_L\rho_R e^{-2\kappa N a}}{(E_F - E_i - \delta)^2 + \gamma^2}. \tag{3}$$

Here $\Gamma_0 = e^2/\pi\hbar$ is the conductance quantum, ρ_L and ρ_R are the spin densities of states of the metal atoms at the left and right interfaces, respectively, $\kappa = a^{-1}\ln\Delta$ is the decay constant, and N is the number of the barrier atoms excluding the impurity. Formula (3) is equivalent to the well-known expression for resonance tunneling,[16] the log-scaling of the decay constant versus the barrier height reflecting the tight-binding approach.[17] As is seen from Eq. (3), the posi-

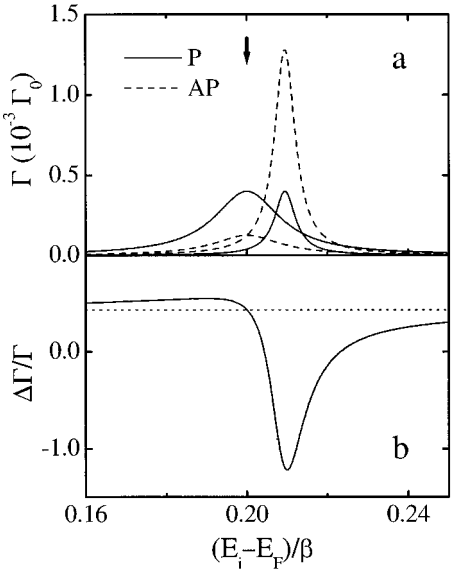

FIG. 1. (a) Spin-resolved conductance for the parallel (solid lines) and antiparallel (dashed lines) magnetization of the electrodes and (b) tunneling magnetoresistance of the 1D magnetic tunnel junction as a function of the on-site atomic energy of the impurity. Parameters of the model are as follows: $N_L=1$, $N_R=4$, $E_b-E_F=10\beta$, $E_m^{\uparrow}-E_F=0$, $E_m^{\downarrow}-E_F=1.9\beta$. The dotted line in (b) shows the value of TMR in the absence of the impurity.

tion of the resonance is shifted from the impurity energy E_i by δ. The shift δ and the width γ of the resonance are determined by the leakage of an electron from the impurity state to the electrodes:

$$\delta \approx -2\beta\Delta^{-1}+\beta^2(e^{-2\kappa N_L a}\,\mathrm{Re}\,G_L+e^{-2\kappa N_R a}\,\mathrm{Re}\,G_R), \tag{4}$$

$$\gamma \approx \beta^2(e^{-2\kappa N_L a}\,\mathrm{Im}\,G_L+e^{-2\kappa N_R a}\,\mathrm{Im}\,G_R). \tag{5}$$

Here G_L and G_R are the Green's functions of the metal atoms at the left and right interfaces, respectively, and N_L and N_R are the number of insulator atoms between the impurity and the metal leads, so that $N_L+N_R=N$. Since the electrodes are ferromagnetic the leakage shift and rate are spin-dependent and, therefore, the position, the width and, consequently, the amplitude of the resonance are also spin-dependent.

This result is illustrated in Fig. 1(a), which shows the calculated spin-resolved conductance of the 1D tunnel junction as a function of the impurity energy. As is seen from this figure, for either the parallel (P) or the antiparallel (AP) magnetization alignment of the electrodes, the two resonant peaks appear at different energies and have different amplitudes and widths. The magnitude of the *spin-independent* shift of the resonance $2\beta\Delta^{-1}$ is determined by the barrier height and is shown in Fig. 1(a) by the arrow. The *spin-dependent* shift of the resonance originates mainly from the coupling to the left electrode since the impurity is much closer to it than to the right. For the parameters chosen, this shift is zero for the majority spins (because $\mathrm{Re}\,G_L^{\uparrow}=0$) and is 0.01β for the minority spins within either the P or AP alignment. It follows from Eqs. (3) and (5) with our assumed asymmetric position of the impurity within the barrier that the amplitude of the resonance is proportional to ρ_R/ρ_L. The peak heights in Fig. 1(a) are, therefore, the same for the two spins within the P alignment, but are different within the AP alignment. The width of the resonance is larger for the majority spins than for the minority spins due to the higher density of states for the former. As is evident from Fig. 1(b), the spin dependence of the position, amplitude, and width of the resonance leads to TMR, the magnitude and the sign of which depend strongly on the impurity energy with respect to the Fermi energy. Far away from the resonance the value of TMR approaches that expected from the well-known Julliere formula[1] [the dotted line in Fig. 1(b)].

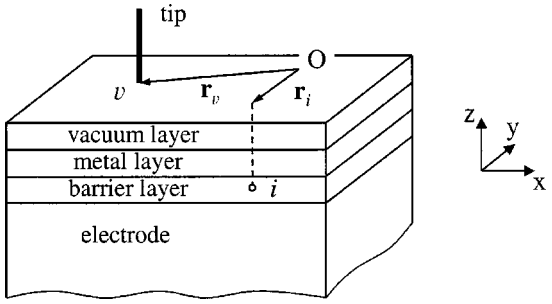

FIG. 2. Geometry in the calculations. The magnetic tunnel junction is infinite in the lateral *xy* direction. An impurity is introduced in the barrier layer at site *i*. Index v denotes the site in the vacuum layer which is coupled to the tip. $\mathbf{r}_v$ and $\mathbf{r}_i$ are the transverse coordinates of sites v and i.

This influence of the impurity on the magnitude and the sign of TMR can be observed by STM. We demonstrate this by calculating the local conductance across a magnetic tunnel junction using a single-band tight-binding model. The MTJ consists of a semiinfinite metal electrode, an insulating barrier layer, and a top ferromagnetic metal layer, as is illustrated in Fig. 2. The electric current is passed to the MTJ from the metal tip through the vacuum layer. The tip is modeled by a semiinfinite monoatomic wire. The vacuum is represented by a few atomic monolayers with the potential E_v which provides no states at the Fermi energy E_F. On-site atomic energies of the barrier and the tip are denoted by E_b and E_t, respectively. The exchange splitting of the spin bands of the ferromagnets is simulated by setting different potentials for the up and down spins, i.e., $E_e^{\uparrow}$ and $E_e^{\downarrow}$ for the electrode and $E_m^{\uparrow}$ and $E_m^{\downarrow}$ for the metal layer. An impurity is introduced substitutionally within the barrier and has an on-site energy E_i. The thickness of the barrier, metal and vacuum layers are denoted by L_b, L_m, and L_v, respectively.

The conductance is evaluated using the Kubo formula Eq. (1), where the local current operator J is taken across the bond between the edge atom of the tip (t) and the adjacent site of the vacuum layer (v), so that $n_1=v$ and $n_2=t$ in Eq. (2). The three matrix elements of the *total* Green's function G_{tt}, G_{vt}, and G_{tv}, therefore, determine the conductance. Using the Dyson equation these can be written in terms of the matrix elements of the Green's function g of the *isolated* tip and the *isolated* MTJ containing the impurity. In particular, $G_{tt}=g_{tt}(1+\beta G_{vt})$, $G_{vt}=G_{vv}\beta g_{tt}$, and G_{vv}

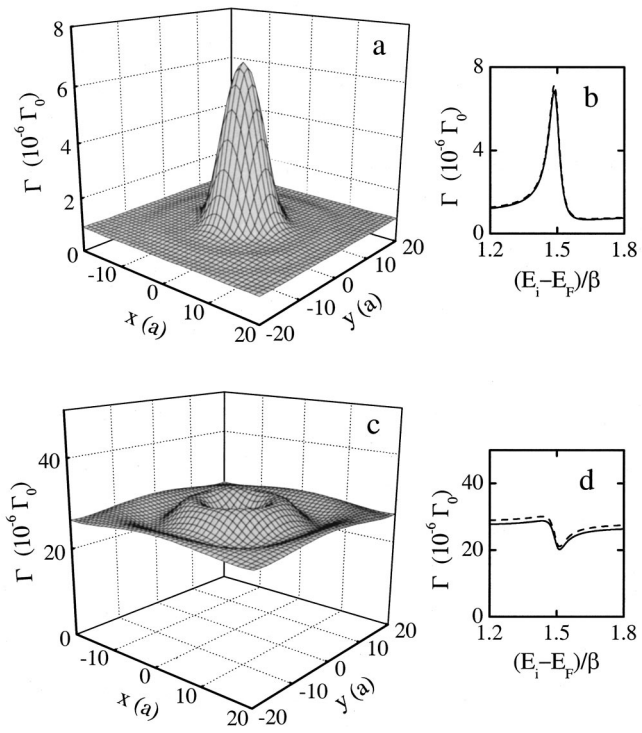

FIG. 3. Lateral distribution of the conductance calculated at $E_i - E_F = 1.49\beta$ for $L_m = 10a$ (a) and $L_m = 20a$ (c) and the respective dependence of the conductance on the impurity energy (b), (d) calculated exactly (solid lines) and using Eq. (7) (dashed lines). Parameters of the model are as follows: $E_t - E_F = 0$, $E_e - E_F = E_m - E_F = 3\beta$, $E_b - E_F = 6.2\beta$, $L_b = 5a$, and $L_v = 10a$.

$= [(g_{vv})^{-1} - \beta^2 g_{tt}]^{-1}$. Thus we need to find the two diagonal matrix elements g_{tt} and g_{vv}. The former is given by $g_{tt} = (\Delta_t - \sqrt{\Delta_t^2 - 1})/\beta$, where $\Delta_t = (E_F - E_t)/2\beta$. The latter may be expressed in terms of the Green's function g^0 for a MTJ that contains no impurity, i.e.,

$$g_{vv} = g^0_{vv} + g^0_{vi} \frac{(E_i - E_b)}{1 - g^0_{ii}(E_i - E_b)} g^0_{iv}. \tag{6}$$

The matrix elements g^0_{ii}, g^0_{vv}, and g^0_{iv} may be found using the standard recursion procedure taking into account the fact that the MTJ with no impurity has periodicity in the lateral directions.[18]

We consider first the simplest case of a *nonmagnetic* tunnel junction, so that $E_e^{\uparrow} = E_e^{\downarrow}$ and $E_m^{\uparrow} = E_m^{\downarrow}$. Figure 3(a) shows the calculated lateral distribution of the conductance as the tip scans an area above the impurity atom, which is placed in the middle of the barrier layer at $x = y = 0$. The striking feature about this figure is the presence of a spike in the conductance distribution at $x = y = 0$. As is seen, the value of the conductance for the tip positioned above the impurity is an order of magnitude higher than far away from it. This spike originates from electrons traversing ballistically the top metallic layer and, then, tunneling resonantly across the barrier via the localized electronic state in the band gap of the insulator. The ability to detect the impurity through the top metal layer is due to tunneling across the vacuum, since this selects

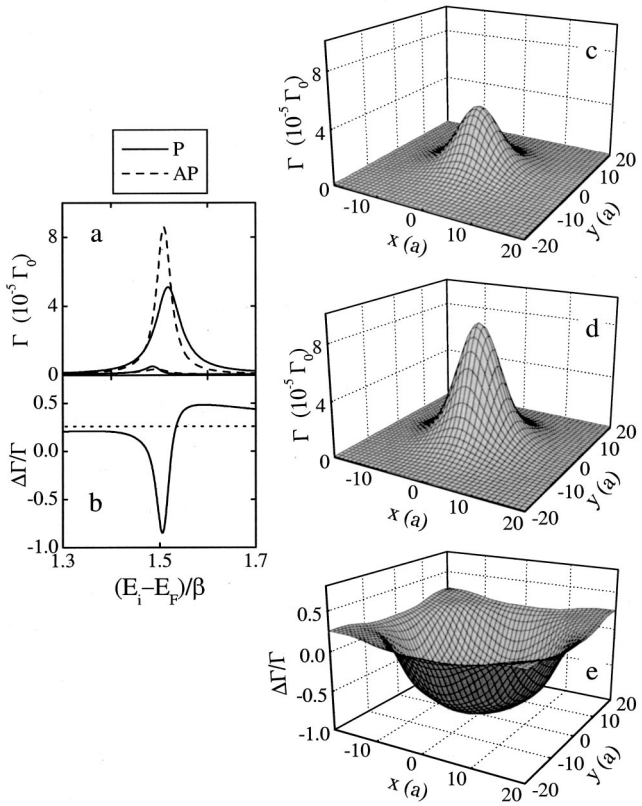

FIG. 4. (a) Spin-resolved conductance for the parallel (P) and antiparallel (AP) configurations of the MTJ and (b) TMR versus impurity energy. Lateral distribution of the conductance for the P (c) and AP (d) magnetic configurations and lateral variation of TMR (e) calculated for $E_i - E_F = 1.51\beta$. The dotted line in (b) shows the value of TMR at off-resonance conditions. Parameters of the model are as follows: $E_t - E_F = 0$, $E_b - E_F = 6.2\beta$, $E_e^{\uparrow} - E_F = E_m^{\uparrow} - E_F = 3\beta$, $E_e^{\downarrow} - E_F = E_m^{\downarrow} - E_F = 4\beta$, $L_b = 5a$, and $L_m = L_v = 10a$.

electrons in a relatively narrow angular window close to normal incidence. The diameter of the spike is, therefore determined by the contribution from nonzero transverse momenta to the conductance. By varying the parameters of the model in realistic limits we found that the diameter of the spike varies within $10a - 20a$.[19]

The resonant character of the tunneling process is evident from Fig. 3(b), which shows the calculated conductance as a function of the on-site atomic energy of the impurity. The asymmetry of the resonance seen in this figure is a consequence of the Fano effect,[20] which originates from the interference between direct and resonant tunneling (e.g., Ref. 21). In our case this asymmetry can be exhibited explicitly in a simplified expression for the conductance. Assuming weak tip MTJ coupling, the conductance is approximated by $\Gamma \approx \Gamma_0 4\pi^2 \beta^2 \rho_t \rho_v$, where ρ_t and ρ_v are the density of states of the isolated tip and the isolated MTJ containing the impurity. Making use of Eq. (6) for evaluating ρ_v, we arrive at

$$\Gamma \approx \Gamma_0 4\pi^2 \beta^2 \rho_t \rho^0_v \left\{ 1 + p \frac{1 + qE}{E^2 + 1} \right\}, \tag{7}$$

where ρ^0_v is the density of states at site v of the isolated MTJ without impurity, $E = (E_F - E_i - \mathrm{Re}\,\Sigma)/\mathrm{Im}\,\Sigma$ is the reduced

energy, Σ is the self-energy at the impurity site which is defined by $g_{ii}^0=(E_F-E_b-\Sigma)^{-1}$, $p=(E_i-E_b)(E_F-E_b-\mathrm{Re}\,\Sigma)\mathrm{Re}[(g_{iv}^0)^2]/(\pi\rho_v^0\,\mathrm{Im}\,\Sigma)$ is the relative amplitude of the resonance, $q=\mathrm{Im}[(g_{iv}^0)^2]/\mathrm{Re}[(g_{iv}^0)^2]$ is the asymmetry parameter, and where we have assumed that $|\Sigma|\ll|E_F-E_b|$. The first term in Eq. (7) describes the direct tunneling and the second term is responsible for the resonant process. As is seen from Fig. 3(b), the simplified expression (7) gives an accurate representation of the conductance, the resonance amplitude and asymmetry being $p\approx 6.1$ and $q\approx -0.4$.

A strong direct tunneling contribution can make the conductance over the impurity site lower than away from it. This is illustrated in Fig. 3(c), where we have chosen a top metal layer thickness $L_m=20a$, for which the magnitude of the direct tunneling is 20 times greater than that for $L_m=10a$ due to the presence of a quantum-well state. In this case when the tip is positioned above the impurity, the amplitude of the resonance becomes negative, $p\approx -0.2$, and thus the resonant tunneling manifests itself as an antiresonance [Fig. 3(d)]. The interference between the direct and resonant channels leads to lateral oscillations in the conductance, which are evident from Fig. 3(c) and reflect the oscillations in $\mathrm{Im}[(g_{iv}^0)^2]$ as a function of the tip position v.

Finally, we consider the effect of the impurity on the local TMR by allowing both the metal layer and the electrode to be ferromagnetic with exchange-split bands $E_e^{\uparrow}=E_m^{\uparrow}$ and $E_e^{\downarrow}=E_m^{\downarrow}$. The results of the calculations, which are displayed in Fig. 4(a), demonstrate that the resonant peaks are shifted relative to each other and have different amplitudes and widths for the parallel and antiparallel magnetic configurations of the MTJ. This leads to the variation of TMR versus the on-site atomic energy of the impurity as shown in Fig. 4(b). The sensitivity of the TMR to the impurity energy is similar to that predicted within the 1D model [compare to Fig. 1(b)]. However, the 3D geometry of Fig. 2 allows us also to predict the lateral distribution of the conductance and TMR. Setting $E_i-E_F=1.51\beta$, at which a maximum inverse TMR is expected [see Fig. 4(b)], Figs. 4(c) and 4(d) demonstrate that the amplitude of the spike in the conductance distribution is a factor of 2 larger for the antiparallel configuration than for the parallel configuration. As is evident from Fig. 4(e), this leads to a strong negative value of TMR when the tip is directly above the impurity, compared to a smaller positive value away from the impurity.

In conclusion, we have shown that the local TMR in an MTJ is very sensitive to the electronic state of the impurity within the barrier layer and to the lateral position of the tip, which is used to probe the conductance. These effects occur due to the spin-dependent resonance in the impurity-assisted tunneling. The predicted dramatic lateral variation in TMR across the impurity atom could be detected by STM.

The research was funded by Hewlett Packard Laboratories, Palo Alto, through a collaborative research program. The authors are thankful to Victor Burlakov, Bret Heinrich, Dimitris Kechrakos, and Wulf Wulfhekel for useful discussions. The computations were performed in the Materials Modelling Laboratory at the Department of Materials, University of Oxford.

[1] M. Julliere, Phys. Lett. A **54**, 225 (1975).
[2] J. S. Moodera, L. R. Kinder, T. M. Wong, and R. Meservey, Phys. Rev. Lett. **74**, 3273 (1995).
[3] T. Miyazaki and N. Tezuka, J. Magn. Magn. Mater. **139**, L231 (1995).
[4] W. J. Gallagher *et al.*, J. Appl. Phys. **81**, 3741 (1997).
[5] P. M. Levy and S. Zhang, Curr. Opin. Solid State Mater. Sci. **4**, 223 (1999).
[6] J. S. Moodera, J. Nassar, and G. Mathon, Annu. Rev. Mater. Sci. **29**, 381 (1999).
[7] V. Da Costa, Y. Henry, F. Bardou, M. Romeo, and K. Ounadjela, Eur. Phys. J. B **13**, 297 (2000).
[8] E. Y. Tsymbal and D. G. Pettifor, Phys. Rev. B **58**, 432 (1998).
[9] W. H. Butler, X. G. Zhang, T. C. Schulthess, and J. M. MacLaren, Phys. Rev. B **63**, 054416 (2001).
[10] I. I. Oleinik, E. Y. Tsymbal, and D. G. Pettifor, Phys. Rev. B **62**, 3952 (2000).
[11] Ph. Mavropoulos, N. Papanikolaou, and P. H. Dederichs, Phys. Rev. Lett. **85**, 1088 (2000).
[12] W. Wulfhekel, M. Klaua, D. Ullmann, F. Zavaliche, J. Kirschner, R. Urban, T. Monchesky, and B. Heinrich, Appl. Phys. Lett. **78**, 509 (2001).
[13] W. H. Rippard, A. C. Perrella, and R. A. Buhrman, Appl. Phys. Lett. **78**, 1601 (2001).
[14] R. Kubo, J. Phys. Soc. Jpn. **12**, 570 (1957).
[15] P. A. Lee and D. S. Fisher, Phys. Rev. Lett. **47**, 882 (1981).
[16] See, e.g., S. Datta, *Electronic Transport in Mesoscopic Systems* (Cambridge University Press, Cambridge, 1995).
[17] S. Zhang and P. M. Levy, Eur. Phys. J. B **10**, 599 (1999).
[18] T. N. Todorov, Phys. Rev. B **54**, 5801 (1996).
[19] In this calculation we assume that the localized state lies close to the Fermi energy that allows observing a sizable effect at a small STM voltage. In real systems one can expect the presence of impurity/defects levels at various energies within the band gap, which could be sensed by varying the voltage. The effect of the STM voltage is discussed by D. Kehrakos, E. Y. Tsymbal, and D. G. Pettifor, J. Magn. Magn. Mater. (to be published).
[20] U. Fano, Phys. Rev. **124**, 1866 (1961).
[21] A. Schiller and S. Hershfield, Phys. Rev. B **61**, 9036 (2000).